

Postoperative facial appearance of patients with extensive oral squamous cell carcinoma can be adequately preserved with in-house virtually planned mandibular reconstruction

GEORG HOENE¹, NORMAN MOSER¹, BORIS SCHMINKE¹, BERNHARD WIECHENS², ANDREAS LEHA³,
TATJANA KHROMOV⁴, HENNING SCHLIEPHAKE¹ and PHILLIPP BROCKMEYER¹

Departments of ¹Oral and Maxillofacial Surgery and ²Orthodontics, University Medical Center Goettingen, D-37075 Goettingen; ³Institute of Medical Statistics, University Medical Center Goettingen, D-37073 Goettingen; ⁴Institute of Clinical Chemistry, University Medical Center Goettingen, D-37075 Goettingen, Germany

Received May 30, 2023; Accepted September 27, 2023

DOI: 10.3892/mco.2023.2693

Abstract: The present study aimed to assess the concordance of preoperative and postoperative hard and soft tissues in patients with advanced oral squamous cell carcinoma (OSCC) following virtual surgical planning (VSP) mandibular reconstruction. In the present study, a cohort of 32 patients with OSCC underwent in-house VSP, followed by guided mandibular reconstruction utilizing vascularized free tissue grafts sourced from the fibula or scapula. A morphometric analysis was conducted comparing preoperative and postoperative three-dimensional virtual models to evaluate discrepancies and identify potential risk factors associated with poor reconstruction outcomes. The outcome variables were the differences in root mean square (RMS) and mean surface distance (MSD) resulting from the application of an iterative closest point algorithm to the virtual data. The validity of soft tissue comparison data is limited due to its susceptibility to various confounding variables. The present study conducted a comprehensive re-evaluation of these variables. High tumor stage, positive N status and the use of adjuvant therapy contributed to more noticeable differences in preoperative and postoperative facial soft tissue appearance. The accuracy of postoperative bone reconstruction results was higher in patients who underwent neomandibular formation using a fibular graft compared with those who received a scapular graft. Preoperative and postoperative soft tissue analyses were conducted for comparison. The MSD showed a deviation of 3.2 mm (\pm 2.0 mm SD; range 1.3-9.5 mm), whereas the RMS was 5.3 (\pm 2.9 SD; range 2.1-14). In conclusion, in-house VSP

and guided mandibular reconstructions can yield clinically accurate results, preserving patient appearance and offering the advantage of rapid feasibility.

Introduction

Oral squamous cell carcinoma (OSCC) stands as one of the most prevalent malignant neoplasms globally (1). The invasion of OSCC can affect adjacent mandibular bone, necessitating its removal as an integral component of oncologic treatment (2).

Tumor resection is associated with loss of function, such as chewing, swallowing, and speaking, facial aesthetics, and a corresponding reduction in postoperative health-related quality of life (HRQOL) (3). Vascularized free tissue transfer, predominantly sourced from the fibula (4) or scapula (5), is a commonly employed technique for mandible reconstruction, aiming to achieve the optimal balance of functionality and aesthetics in anatomical restoration. This elaborate procedure heavily relies on surgical skill, and there is no consistent standard for shaping the bone graft, rendering it challenging to predict the impact of healing on the patient's postoperative facial appearance (6).

The development of computer-aided virtual surgical planning (VSP), combined with computer-aided design and computer-aided manufacturing (CAD/CAM) for the production of surgical guides for guided surgery, is now considered a standard procedure for mandibular reconstruction and is commercially available (7). These procedures provide the potential for a more precise and customized surgical approach, precise positioning of the vascularized free tissue graft, reduced surgical and graft ischemia time, and improved postoperative esthetic results (8,9). Nonetheless, commercial manufacturing processes can be time consuming, potentially causing delays in tumor therapy (8,10).

VSP and CAD/CAM techniques have become comprehensible and feasible even for individuals not specialized in bioinformatics. Software-based planning solutions such as the Mimics Innovation Suite (Materialise, Leuven, Belgium) or the open-source project Blender (Blender®; Blender Foundation and Institute; Amsterdam, The Netherlands) enable the

Correspondence to: Dr Phillipp Brockmeyer, Department of Oral and Maxillofacial Surgery, University Medical Center Goettingen, 40 Robert-Koch-Straße, D-37075 Goettingen, Germany
E-mail: ph.brockmeyer@gmail.com

Key words: oral squamous cell carcinoma, virtual surgical planning, guided surgery, facial appearance, computer-aided design/computer-aided manufacturing

integration of planning processes directly in clinical settings, facilitating a more adaptable and personalized approach to addressing each patient's requirements within a shorter timeframe.

Three-dimensional (3D) printed models of the VSP can be used to accurately model and pre-bend standardized osteosynthesis plates preoperatively, leading to further time savings during the procedure (7). Moreover, as digital planning determines the position of the bone segments, potential dental rehabilitation options can be discussed with the patient at an early stage of therapy (11). However, it remains uncertain whether in-house VSP and guided surgery can effectively contribute to the restoration of the patient's preoperative facial appearance during the postoperative healing process. The primary objective is not to predict the patient's soft tissue reconstruction. The aim is not to illustrate the planned bone reconstruction and the actual surgery but to show their impact on the existing soft tissues. In the present study, we performed in-house VSP and guided mandibular reconstruction in 32 patients with OSCC using fibular or scapular vascularized free tissue transfer. We evaluated the impact of the outlined procedures on the accuracy of postoperative hard and soft tissue reconstruction and identified risk factors associated with poor outcomes.

Materials and methods

Patients. This retrospective analysis was performed on a cohort of 32 patients diagnosed with locally invasive OSCC. The sample size of 32 was determined using G*Power (v.3.1.9.2; University of Duesseldorf, Duesseldorf, Germany) with a significance level set at 0.05, a power of 0.95, and an estimated large effect size of 0.6. All patients underwent segmental mandibular resection and subsequent reconstruction. No cases involved complete mandibular resection. Among the 32 patients, 26 received a fibular vascularized free tissue transfer. In the remaining six patients, either the extent of soft tissue resection was too extensive for a fibular graft, or vascular supply from the lower leg was deemed unsuitable.

In these cases, a scapular vascularized free tissue transfer from the right shoulder was employed instead. The patient population consisted of 22 male and 10 female individuals, with ages ranging from 47 to 82 years. The clinical characteristics of all patients are detailed in Table I. In assessing baseline clinical characteristics, tumor stages T1 and T2 were grouped together, as well as T3 and T4, while AJCC stages I and II were also grouped together, along with AJCC stages III and IV.

For analysis of nodal status, patients were categorized into two groups: those with lymph involvement (positive) and those without (negative). Other factors evaluated included postoperative adjuvant therapy (radiation and/or drug therapy), the number of graft segments employed for reconstruction, the type of osteosynthesis used (2.0 mm mini-plate osteosynthesis vs. 2.7 mm reconstruction plate osteosynthesis), the duration between preoperative and postoperative control imaging, and the evaluation of postoperative preservation in occlusal support zones.

All participants provided written informed consent for their inclusion in the study, which adhered to principles outlined in the Declaration of Helsinki. Additionally, the study received

review and approval from the local ethics committee of the University Medical Center Goettingen (Goettingen, Germany; approval no. 14/7/19).

In-house VSP and CAD/CAM-based fabrication of surgical guides. Computed tomography (CT) scans of the head-neck-thorax region, performed for initial tumor staging, and angio-CT to evaluate vascular supply of the lower extremity (each with a 0.6 mm slice thickness), were used for VSP. All CT examinations were performed at the Department of Diagnostic and Interventional Radiology, University Medical Center Goettingen, Germany. CTA and CT scans were performed using a third-generation dual-energy CT scanner (SOMATOM Definition AS & Force and SOMATOM Definition AS Edge, Siemens Healthineers, Forchheim, Germany). Virtual planning for all cases was performed by PB or NM, and case analysis was performed by GH. All analyses were performed twice; with the second round of analyses performed at a minimum interval of 5 to 14 days later. The surgical procedure was performed as a collaborative effort by the staff of the Department of Oral and Maxillofacial Surgery at the University of Goettingen, enduring a high professional standard.

The visible mandibular bone defect (resulting from tumor invasion) was virtually resected with a safety margin of 1 cm both anteriorly and posteriorly, as illustrated in Figs. 1C and 2A). Subsequently, the 3D model of the fibula or scapula was inserted into the bone defect to properly reconstruct the external contour of the original jaw segment (Figs. 1A, 1D, 2B and 2C). The individual fibula and scapula segments were virtually osteotomized (Figs. 1B and 2D). A 3D model of the entire reconstructed neomandible was printed using a Monoprice Inventor IIIP 3D printer (Monoprice, California, USA) with PLA material (Polymaker, Houston, USA). For 27 cases, a customized 2.7 mm reconstruction osteosynthesis plate (KLS Martin, Tuttlingen, Germany) was employed, tailored to fit the segments and fixed to the printed model using osteosynthesis screws (KLS Martin, Tuttlingen, Germany). In five cases, 2.0 mm mini osteosynthesis plates from the same manufacturer were utilized as an alternative (KLS Martin, Tuttlingen, Germany).

The osteosynthesis plates were digitally segmented from the CBCT DICOM data set, and the resulting 3D model was inserted into the VSP (Fig. 1D). Subsequently, two surgical guides for the mandibular osteotomies (one for the anterior and one for the posterior) and a graft guide for the fibula/scapular osteotomies were fabricated using an in-house CAD/CAM-based procedure (Figs. 1B, 1C, 2A and 2D). All VSP steps were performed using the Mimics In-novation Suite software (Materialise, Leuven, Belgium). The final surgical guides were 3D printed from surgical guide resin (FormLabs, Massachusetts, USA) using the FormLabs Form 3B+ 3D printer (FormLabs, Massachusetts, USA) and sterilized. The pre-bent osteosynthesis plates were sterilized and prepared for surgery.

Guided mandibular reconstruction. Following the initial neck dissection (selective level 1-3, with more if needed) and cervical vascular preparation for vascularized free tissue transfer, mandibular resection was performed during intraoral tumor resection. The affected mandibular segment was exposed, and

Table I. Patient clinical baseline characteristics.

N	Age at surgery, years	Sex	pT	pN	M	G	Stage	AT	Tx	Segments	Plate	OS	TBC, days
1	75	F	3	2b	0	3	III	+	Fibula	2	Mini	+	174
2	53	M	3	0	0	1	III	+	Fibula	1	Mini	+	162
3	65	M	4	0	0	1	IVA	+	Fibula	2	Mini	+	279
4	47	F	4	2b	0	3	IVA	+	Fibula	3	Mini	+	244
5	58	M	1	0	0	2	I	-	Fibula	2	Mini	-	197
6	78	M	2	2a	0	2	IVA	+	Fibula	2	Reco	+	230
7	51	M	1	0	0	2	I	-	Fibula	2	Reco	-	116
8	67	M	4	0	0	2	IVA	+	Fibula	2	Reco	+	188
9	66	M	3	0	0	2	III	+	Fibula	2	Reco	-	157
10	51	M	3	1	0	2	III	+	Fibula	3	Reco	-	225
11	81	F	4	0	0	2	IVA	+	Fibula	3	Reco	+	325
12	75	F	1	0	0	2	I	-	Fibula	2	Reco	-	49
13	68	M	2	0	0	2	II	-	Fibula	2	Reco	-	204
14	66	M	2	0	0	2	II	-	Fibula	3	Reco	-	287
15	65	M	4	2b	0	2	IVA	+	Fibula	3	Reco	+	168
16	58	M	2	0	0	2	II	-	Fibula	2	Reco	-	336
17	66	F	2	1	0	2	III	+	Fibula	2	Reco	-	354
18	76	M	2	0	0	2	II	-	Fibula	1	Reco	-	290
19	65	F	4	0	0	2	IVA	+	Fibula	3	Reco	+	157
20	58	M	3	2b	0	3	IVA	+	Fibula	2	Reco	-	43
21	73	M	2	2b	0	2	IVA	+	Fibula	2	Reco	+	251
22	54	F	4	2b	0	2	IVA	+	Fibula	2	Reco	+	200
23	70	M	1	0	0	1	I	-	Fibula	1	Reco	-	188
24	56	M	4	2c	0	2	IVA	+	Fibula	3	Reco	-	268
25	76	F	2	0	0	2	II	-	Fibula	2	Reco	+	189
26	53	M	4	0	0	2	IVA	+	Fibula	3	Reco	+	197
27	63	F	4	3b	0	2	IVB	+	Scapula	2	Reco	-	45
28	62	F	4	2c	0	2	IVA	+	Scapula	2	Reco	-	168
29	62	F	4	3b	0	3	IVB	+	Scapula	1	Reco	-	248
30	77	M	4	3b	0	2	IVB	+	Scapula	2	Reco	-	Mis
31	60	M	4	3b	0	3	IVB	+	Scapula	2	Reco	-	Mis
32	82	M	3	2b	0	3	IVA	+	Scapula	1	Reco	-	884

F, female; M, male; AT, adjuvant therapy; Tx, transplant; OS, postoperative occlusal supporting zones; TBC, time between CT scans; Mis, missing value; Mini, mini osteosynthesis plates; Reco, reconstruction osteosynthesis plate.

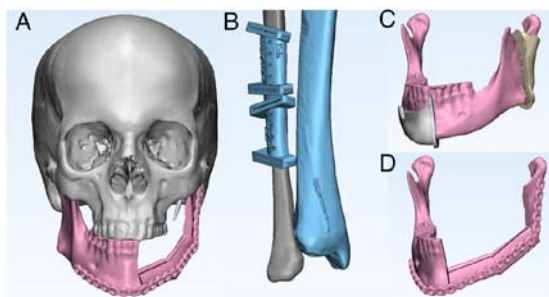


Figure 1. (A) Final virtual surgical planning (skull with neomandible), (B) fibula and tibia with corresponding transplant guide, (C) preoperative mandible with corresponding surgical guide for tumor resection, (D) final virtual planned neomandible with pre-bented osteosynthesis plate for fibula segment fixation.

the surgical guides (anterior and posterior resection planes) were positioned and fixed to the mandible. The mandible was then osteotomized along the predetermined planes using a jigsaw. Screw holes for the pre-bent osteosynthesis plate were predrilled using shafts modeled in surgical guides. The entire primary OSCC (soft tissue with attached mandibular bone) was sent for pathology, and marginal sections were taken and submitted for frozen section analysis. Defect reconstruction was performed only in the case of R0 resection.

In parallel, the fibula harvest was performed using a two-team approach. When the bony fibula was visualized and the vascular pedicle (A./V. fibularis) was identified, the fibula was pre-osteotomized using the jigsaw, and the graft guide was positioned over the vascular perforator with the attached

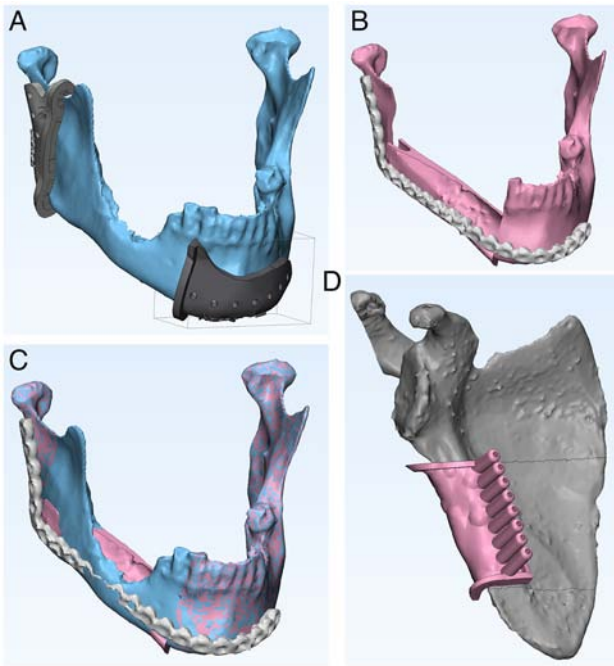


Figure 2. (A) Preoperative mandible with corresponding surgical guide for tumor resection, (B) final virtual planned neomandible with pre-bent osteosynthesis plate for scapula segment fixation, (C) combined and matched simulations pre- and postoperatively, (D) scapula with corresponding transplant guide positioned on the margo lateralis.

skin island. The guide was secured with osteosynthesis screws, and the individual segments were osteotomized using a jigsaw while protecting the vascular pedicle in predetermined planes. Subsequently, the individual fibular segments were screwed to the pre-bent osteosynthesis plates.

The 3D-arranged bone graft with an attached vascular pedicle was transferred to the head and secured in place through the predrilled holes in the fibular segments. The skin island was sutured into the soft tissue defect, and the vascular pedicle was directed cervically for microvascular reanastomosis, performed with the aid of an operating microscope (Carl Zeiss Meditec, Oberkochen, Germany).

In cases involving scapular harvesting, following the necessary intraoperative repositioning and visualization of the bony scapula and vascular pedicle, the scapula was pre-osteotomized from the margo lateralis, inverted, and the cutting guide was securely attached to the scapular segment from below using osteosynthesis screws, as illustrated in Fig. 2D. The predetermined segments were subsequently osteotomized using the jigsaw, and the segment was fixed to the pre-bent osteosynthesis plate in accordance with the fibula procedure.

Morphometric evaluation. Postoperative control CT scans (0.6 mm slice thickness) were imported into the Mimics suite software (Materialise, Leuven, Belgium), and virtual 3D models were generated through semi-automatic thresholding and tessellation. A fixed threshold range of -700 to +2,200 was applied for soft tissues, while a threshold range of +300 to the highest was used for bony structures.

The 3D models were imported into the 3-Matic software (Materialise, Leuven, Belgium), where the trimming function was used to remove existing artifacts (e.g., caused by dental

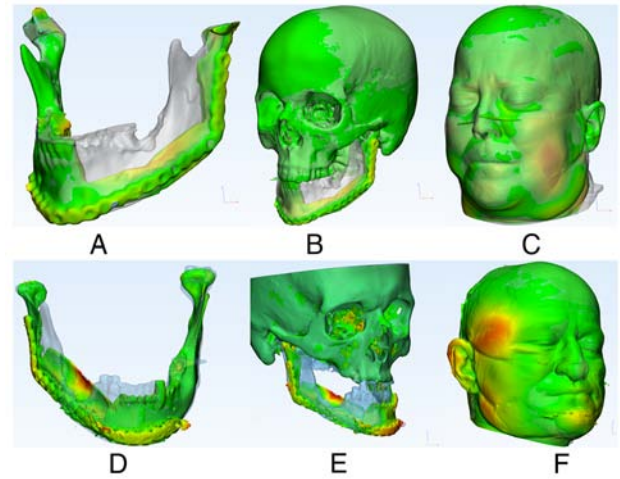


Figure 3. (A) Overlay (with heat map) of the preoperative mandible with postoperative reconstruction result of fibula transplant; (B) overlay (with heat map) of the preoperative and postoperative skull of fibula transplant; (C) overlay (with heat map) of the preoperative and postoperative soft tissue appearance of fibula transplant; (D) overlay (with heat map) of the preoperative mandible with postoperative reconstruction result of scapula transplant; (E) overlay (with heat map) of the preoperative and postoperative skull of scapula transplant; (F) overlay (with heat map) of the preoperative and postoperative soft tissue appearance of scapula transplant; the heat map colors between red and green indicate deviations of the two 3D data sets between 0 (green) and 10 (red) in millimeters.

crowns). The models were aligned using the classical Iterative Closest Point (ICP) algorithm and overlapping regions were evaluated using the 3-Matic Part Comparison Analysis function. This function calculates the distance between closed points among the surface triangles of 3D surface mesh and automatically aligns and calculates the deviations between the corresponding point pairs. The surface deviations are visualized in a heatmap. The analysis provides values for the mean deviation of the same mesh surface points (MSD=Mean Surface Distance), along with the associated standard deviation (SD) and root mean square (RMS) values. The exact RMS value was calculated using the following equation:

$$RMS = \sqrt{\frac{1}{2} \sum_{i=1}^n x_i^2}$$

If point Y in the postoperative 3D surface mesh has the closest point Y' in the preoperative 3D surface mesh, then Xn is the distance between Y and Y', where n denotes the total number of point pairs in both 3D surface meshes. The RMS value represents the sum of the averaged 3D deviations and functions as an indicator of the extent to which the deviations between the two individual datasets deviate from zero (12). An example of the generated heatmaps is depicted in Fig. 3A-F for further illustration.

Statistical analysis. All variables, including clinical data and 3D model analysis, were summarized as absolute and relative frequencies or mean ± SD and median (minimum; maximum), as appropriate. The impact of the type of osteosynthesis (reconstruction plate osteosynthesis vs. mini-plate osteosynthesis) on reconstruction accuracy was assessed by employing separate linear models for all reconstruction measures, with the type of osteosynthesis serving as the predictor. Model improvement

Table II. Descriptive data of the part comparison analysis.

Parameter	All cases (n=32)	Fibula cases (n=26)	Scapula cases (n=6)
MSD skull			
Mean ± SD	0.76±0.31	0.68±0.24	1.14±0.3
Median (min; max)	0.68 (0.33; 1.5)	0.61 (0.33; 1.26)	1.1 (0.74; 1.51)
MSD mandible			
Mean ± SD	1.5±0.5	1.31±0.34	2.15±0.55
Median (min; max)	1.4 (0.85; 3.2)	1.14 (0.34; 0.85)	2.06 (1.68; 3.23)
MSD soft tissue			
Mean ± SD	3.2±2.0	2.87±1.83)	5.52±1.48
Median (min; max)	2.3 (1.3; 9.5)	2.26 (1.27; 9.46)	5.21 (4.07; 7.56)
Missing	2	0	2
RMS skull			
Mean ± SD	1.8±0.8	1.64±0.64	2.44±1.07
Median (min; max)	1.6 (0.91; 4.5)	1.43 (0.91; 3.21)	2.02 (1.57; 4.48)
RMS mandible			
Mean ± SD	2.3±0.8	2.08±0.62	3.06±0.94
Median (min; max)	2.2 (1.2; 4.9)	1.88 (1.18; 3.23)	2.75 (2.39; 4.94)
RMS soft tissue			
Mean ± SD	5.3±2.9	4.92±2.77	7.83±3.04
Median (min; max)	4.1 (2.1; 14)	4.04 (2.12; 13.87)	8.47 (3.62; 10.74)
Missing	2	0	2

MSD, mean surface distance; RMS, root mean square.

was assessed through likelihood ratio tests on models where osteosynthesis type was not considered as a predictor. The resulting p-values were corrected for multiple testing using Holm's procedure.

Similar examinations were conducted for all other potential risk factors affecting reconstruction quality. To account for the influence of osteosynthesis type, osteosynthesis type was included as an additional predictor in the linear models. Alongside the results of the likelihood ratio tests, the coefficients from the resulting model fits are presented with 95% confidence intervals and their associated p-values.

Due to the screening nature of this study, unadjusted p-values are reported. A significance level of alpha=5% was set for all statistical tests, and all analyses were performed using the statistical software R (version 4.1.2; R Core Team 2021). The R package ordinal [version 2019.12.10; (13)] was utilized for the ordinal regression model, while the R package logistf [version 1.24.1; (14)] was employed for the Firth correction in the logistic regression models.

Results

3D performance analysis. Descriptive data for the part comparison analysis, aimed at assessing the reconstruction's accuracy in comparison to the preoperative baseline, are shown in Table II. Regarding the 3D morphometric evaluation, data were collected from all 32 cases, and they are presented separately for the 26 fibula cases and all 6 scapula cases.

The analysis revealed deviations between preoperative and postoperative data. The smallest differences in MSD were observed in the whole skull comparison. In this comparison, the majority of the bone tissue remained unaffected by the surgery, and thus maintaining consistency postoperatively. In the mandible analysis, a mean deviation of 1.5 mm was observed, which exceeded the data for the entire skull. The largest mean deviation in the MSD was seen in the soft tissue comparison, where a mean of 3.2 mm was measured.

Two scapula cases could not be evaluated for soft tissue appearance due to the patients' absence at the 6-month control CT scan. Consequently, the postoperative CT scan at two weeks was utilized for the analysis of the skull and mandible.

Factors influencing reconstruction precision. Potential risk factors, such as sex, age at surgery, adjuvant therapy performed, occlusal support zone after surgery, number of segments transplanted, AJCC stage, nodal status, T stage, graft type, time between preoperative and first postoperative follow-up CT scan, and type of osteosynthesis, were examined to identify possible associations with one of three reconstruction accuracy measures (RMS cranial, RMS mandible, RMS soft tissue). Linear models were employed to fit the reconstruction accuracy measure, with the risk factor serving as a predictor. Table III shows the combinations of reconstruction and risk factors where the risk factor significantly improved the model's predictive ability. Table IV provides details on the model fits that underlie these results.

Table III. Combinations of risk factors and reconstruction accuracy measures where the inclusion of the risk factor significantly improved the model prediction of the reconstruction accuracy in linear models.

Risk factor	Reconstruction	P-value
Type of transplant	RMS skull	0.033 ^a
Type of transplant	RMS mandible	0.006 ^b
Adjuvant therapy	RMS soft tissue	0.036 ^a
AJCC stage	RMS soft tissue	0.036 ^a
Nodal status	RMS soft tissue	0.033 ^a

The table shows the reconstruction accuracy measure, the risk factor, and the unadjusted P-value from likelihood ratio tests between the model with and without the risk factor. ^aP<0.05, ^bP<0.01. RMS, root mean square.

The findings from this screening analysis indicate that the type of bone graft used for neo-mandible formation (fibula vs. scapula) is a potential risk factor affecting reconstruction accuracy. Patients who underwent scapular grafts had significantly higher deviations between preoperative baseline data and postoperative reconstruction results. Moreover, high AJCC stage (III and IV), positive nodal status (N+), and the use of adjuvant therapy are likely risk factors associated with poorer postoperative soft tissue reconstruction outcomes. The different osteosynthesis plate systems used for osteosynthetic neomandible fixation do not affect the accuracy of fit. This is despite a 0.7 mm difference in plate diameter.

Discussion

The destruction of the bony mandible resulting from the progression of OSCC can have a significant effect on patients' abilities related to speech, chewing, swallowing, facial appearance, and their overall health-related quality of life (HRQOL) (15). In addition to oncologic considerations, achieving functional and esthetic restoration and facilitating social reintegration are essential objectives of treatment.

Mandibular reconstruction involving vascularized free tissue transfer is a surgically challenging and time-consuming procedure. Therefore, the use of VSP and guided surgery should contribute to increased efficiency, as well as enhance predictability and precision in the outcomes (16).

In the present study, we evaluated the effect of in-house VSP and guided mandibular reconstruction on reconstruction accuracy, specifically examining deviations in the patient's preoperative and postoperative hard and soft tissue appearance. Case study examples of the procedures conducted are depicted in Figs. 4 and 5, showcasing both fibular and scapular bone graft cases, respectively. The patient population under investigation comprised 22 males and 10 females, with a mean age of 65 years (ranging from 47 to 82 years). This demographic profile is in line with other OSCC patient collectives described in the literature (2,6), making it a representative sample.

The fibular free flap was primarily employed for neomandibular reconstruction (81%), followed by the scapular free flap (19%), aligning with findings reported by others (17).

Mandibular reconstruction is most commonly required in patients with advanced T4 tumor stage, accounting for 44% of all patients. This can be readily attributed to the tendency of T4 tumors to infiltrate adjacent structures, necessitating mandibular bone replacement more frequently (18,19). While malignant bone infiltration by tumor cells is rare in early-stage tumors, small tumors near the mandible may require resection and reconstruction to achieve a tumor-free margin as part of the oncologic treatment approach.

We identified potential confounding factors that could have an impact on both reconstruction accuracy and postoperative appearance of facial soft tissue. Higher tumor stages (AJCC stages III and IV) are associated with poorer preoperative and postoperative soft tissue appearance. This association can be partly attributed to the fact that patients at these stages experience considerably greater tissue deficits after resection, necessitating more extensive and complicated reconstruction procedures. Ritschl *et al* reported a poorer level of concordance between VSP data and postoperative reconstruction for higher grade defects in contrast to smaller reconstruction defects (8).

Our findings revealed an association between positive nodal status (N+) and poorer postoperative facial soft tissue appearance, aligning with the results reported by Lee *et al* (20). This association may be attributed to the relationship between positive nodal status, higher tumor stage, and concomitant adjuvant therapy.

Our findings revealed that adjuvant therapy also has a negative effect on postoperative facial appearance. It should be noted that patients with an oncologic indication for adjuvant therapy usually have more advanced tumor disease, necessitating more extensive mandibular reconstruction and, consequently, carrying a higher potential for error. Furthermore, it is worth noting that radiotherapy may affect the processes of soft tissue remodeling, with cases of scarring and complex inflammatory processes documented in the literature (21). These effects could potentially affect the postoperative facial appearance. This side effect is also visible in Fig. 3F, where there is a deviation in the right temporal region. This deviation was not initially associated with the surgery but was still affected by swelling that persisted six months after surgery.

Our data suggest that the type of bone graft used for neomandible formation significantly impacts the quality of postoperative reconstruction. Significantly higher deviations in hard tissue data between preoperative and postoperative states were observed in patients who underwent mandibular reconstruction with a scapular graft compared to those who received a fibular graft. To the best of our knowledge, there are no comparable studies in the literature. This could potentially be attributed to the greater complexity involved in the guided shaping of the scapular flap compared to a fibular flap, primarily due to the adherent musculature and the associated potential for error in positioning the graft guide on the lateral margo. Furthermore, a critical consideration for opting for the scapular flap is the presence of a substantial soft tissue defect, which is a significant factor to bear in mind when assessing the quality of the postoperative reconstruction. Regarding the analysis of the number of bone segments utilized for neo-mandible reconstruction, our findings revealed that the majority of mandibular defects can be replaced with two bone segments.

Table IV. Selected model coefficient; CI and P-values from the multivariate analysis model (likelihood ratio tests).

Reconstruction	Risk factor	Term	Modeled value estimation	CI	P-value
RMS skull	Transplant	Reference value	1.473	[0.80; 2.15]	<0.001 ^a
		Type of transplant (scapula)	0.7675	[0.07; 1.47]	0.033 ^b
		Type of transplant (scapula)	0.2005	[-0.55; 0.95]	0.59
RMS mandible	Transplant	Reference value	1.995	[1.36; 2.63]	<0.001 ^a
		Type of transplant (scapula)	0.9619	[0.30; 1.62]	0.006 ^c
		Type of osteosynthesis (reconstruction osteosynthesis plate)	0.09915	[-0.61; 0.81]	0.777
RMS soft tissue	Adjuvant therapy	Reference value	5.925	[3.3; 8.53]	<0.001 ^a
		No adjuvant therapy	-2.463	[-4.8; -0.17]	0.036 ^b
		Type of osteosynthesis (reconstruction osteosynthesis plate)	0.1446	[-2.7; 2.97]	0.917
RMS soft tissue	AJCC stage	Reference value	3.461	[0.31; 6.60]	0.033 ^b
		AJCC stage III/IV	2.463	[0.17; 4.80]	0.036 ^b
		Type of osteosynthesis (reconstruction osteosynthesis plate)	0.1446	[-2.68; 3.00]	0.917
RMS soft tissue	Nodal status	Reference value	4.515	[1.8; 7.20]	0.002 ^c
		Positive nodal status	2.292	[0.2; 4.40]	0.033 ^b
		Type of osteosynthesis (reconstruction osteosynthesis plate)	-0.426	[-3.2; 2.40]	0.758

For each term in each of the models the table shows the model coefficients with 95% CI and associated P-value. ^aP<0.001, ^bP<0.05 and ^cP<0.01. CI, confidence interval RMS, root mean square.

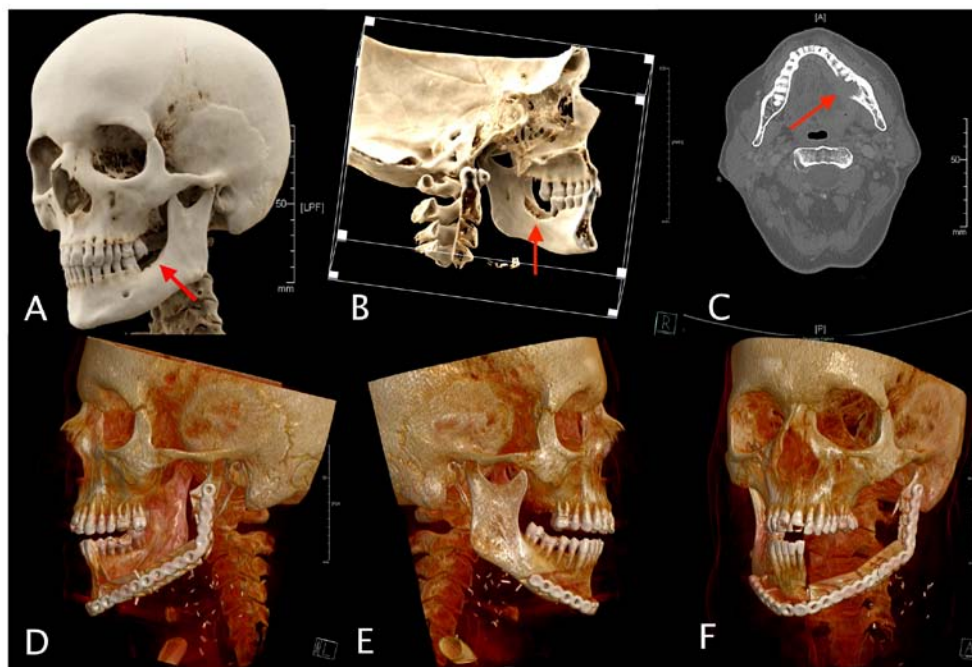


Figure 4. (A) Patients' preoperative skull lateral view using cinematic rendering the red arrow shows the bone defect caused by malignant OSCC invasion; (B) lingual view; (C) axial CT scan layer red arrow showing OSCC invasion; (D) postoperative CT scan after tumor resection and mandibular reconstruction using a free fibula two-segment graft after in-house VSP and guided surgery, cinematic rendering technique, view from the left side; (E) postoperative CT scan, view from the right side; (F) postoperative CT scan, median view.

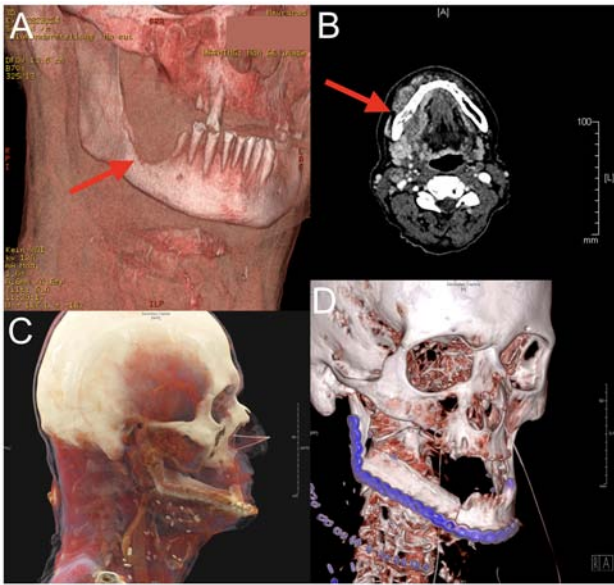


Figure 5. (A) Patient preoperative skull view using cinematic rendering, the red arrow shows the bone defect caused by malignant OSCC invasion (B) axial CT scan layer red arrow showing OSCC invasion; (C) postoperative CT scan after tumor resection and mandibular reconstruction using a free scapula one-segment graft after in-house VSP and guided surgery, cinematic rendering technique. (D) Second view of postoperative CT scan after tumor resection.

There is currently no available literature addressing the impact of the osteosynthesis type (one reconstruction plate vs. multiple mini plates) on the postoperative reconstruction accuracy. In our study, we did not observe a significant influence of the osteosynthesis type on the quality of postoperative reconstruction. What has been thoroughly studied in the literature, however, is the impact of the osteosynthesis type on postoperative complications, such as plate infection, plate fracture, pseudoarthrosis, loosened osteosynthesis screws, or exposed osteosynthesis material (22).

López-Arcas *et al* (23) and van Gemert *et al* (24) did not observe any differences in the aforementioned complications. However, Al-Bustani *et al* proposed an increased complication rate when employing mini-plate osteosynthesis for neomandible reconstruction (25). In contrast, patient-specific implants (PSIs) have demonstrated higher reconstruction accuracy and better fit compared to manually shaped plates (26).

The VSP and guided surgery evaluated in this study are based on an in-house developed and established procedure. A disadvantage of existing commercially available reconstruction procedures using PSIs is that the processing time can extend to several weeks in certain cases. However, due to tumor progression, rapid surgery becomes imperative. Utilizing the in-house procedure outlined here allows for expedited tumor surgery, followed by precise virtual planned mandibular reconstruction. Besides the time-saving aspect mentioned earlier, it's essential not to overlook the cost-benefit ratio. This aspect has been thoroughly explored by Rommel *et al* (27) and Tarsitano *et al* (28), although it was not the primary focus of this study.

This study aims to introduce a new digital algorithm designed to render the analysis of 3D reconstruction more objective. Barr *et al* clearly describe the problem of defining

the reconstruction accuracy (29). Various studies have endeavored to analyze the reconstruction accuracy through metric analyses involving distance and angles (30,31). Unfortunately, this type of evaluation overlooks the complexity of 3D factors and fails to acknowledge the potential for magnified errors. A meta-analysis conducted by Serrano *et al* underscores the necessity for a unified analysis of guided reconstructions to increase comparability (9). In the present collective, the mean MSD of the mandible was 1.5 mm (± 0.5 mm SD; range 0.85 -3.2 mm). The MSD for the cranial data was 0.76 mm (± 0.31 mm SD; range 0.33 -1.5 mm), and the RMS values were 2.3 for the mandibular data (± 0.8 SD; range 1.2-4.9) and 1.8 for the cranial data (± 0.8 SD; range 0.91-4.5).

Comparative data in the literature are still limited. Studies conducted by Ritschl *et al* (8) and Moe *et al* (32) employed similar assessment approaches (8,32). In Moe *et al*'s study, which involved a cohort of 26 cases (24 fibulas and two scapulas), the average MSD values for the mandible were 1.9 mm, accompanied by an associated RMS value of 3.72. Ritschl *et al* reported MSD values of 0.5 mm (range 0.6-6.1) and RMS values of 2.2 (range 1.5-11.1) when comparing mandibles from preoperative 3D models with postoperative 3D models. The data from both studies align closely with the present analysis. When comparing the pre- and postoperative status of the patients regarding the soft tissue relevant to the facial appearance, the points exhibited an average of 3.2 mm (± 2.0 mm SD; range 1.3 -9.5 mm). The corresponding the RMS value was 5.3 (± 2.9 SD; range 2.1-14).

As elucidated earlier, achieving consistent analysis of VSP and guided mandibular reconstruction is difficult. It is imperative to assess the accuracy of the virtual planning, surgical guide fabrication, and postprocessing protocols at each step. This diligence ensures that accuracy is maintained throughout the process and that potential errors within this multi-step protocol do not accumulate and introduce bias into the study results. Hence, all materials used in this study were produced in accordance with strict manufacturer specifications, encompassing the manufacturing process, assembly, and sterilization of the guides. However, it's worth noting that this study has other limitations, primarily stemming from the unequal distribution of group sizes.

It's important to emphasize that 3D models were generated using CT data with a slice thickness of 0.6 mm. In most cases, only positive data in favor of VSP and guided surgery are published, while negative results are often interpreted as an absence of correlation (9). Therefore, there is a need for large, randomized studies to gain a deeper understanding of the complexity involved in a 3D anatomical reconstruction approach.

In conclusion, high tumor stage, positive nodal status, and the use of adjuvant therapy contribute to more substantial deviations in the preoperative and postoperative facial soft tissue appearance among OSCC patients. Differences between preoperative hard tissue data and postoperative reconstruction outcomes are greater in patients who underwent a scapular free flap for neomandible formation compared to those who received a fibular flap. In-house VSP and guided mandibular reconstruction can deliver satisfactory clinical results and can be performed quickly, enabling patients with advanced OSCC to benefit from this technology.

Acknowledgements

Not applicable.

Funding

No funding was received.

Availability of data and materials

The datasets used and/or analyzed during the current study are available from the corresponding author on reasonable request.

Authors' contributions

GH and PB designed the present study. GH, NM, BS and BW collected all the data. GH, AL and PB analyzed and interpreted all data and confirmed the authenticity of all the raw data. GH, TK and PB were instrumental in drafting the manuscript. AL and HS made substantial contributions to the analysis and interpretation of the data. TK and HS made substantial contributions to the conception and design of the study and revised the manuscript. All authors read and approved the final version of the manuscript.

Ethics approval and consent to participate

The study was conducted in accordance with the tenets of the Declaration of Helsinki and reviewed and approved by the local ethics committee of the University Medical Center Goettingen (Goettingen, Germany; approval no. 14/7/19). Written informed consent was obtained from all subjects involved in the study.

Patient consent for publication

All patients gave written informed consent for publication.

Competing interests

All authors declare that they have no competing interests.

References

- Bray F, Ferlay J, Soerjomataram I, Siegel RL, Torre LA and Jemal A: Global cancer statistics 2018: GLOBOCAN estimates of incidence and mortality worldwide for 36 cancers in 185 countries. *CA Cancer J Clin* 68: 394-424, 2018.
- Verhelst P-J, Dons F, Van Bever PJ, Schoenaers J, Nanhekhan L and Politis C: Fibula free flap in head and neck reconstruction: Identifying risk factors for flap failure and analysis of postoperative complications in a low volume setting. *Craniofacial Trauma Reconstr* 12: 183-192, 2019.
- van Beek FE, Jansen F, Mak L, Lissenberg-Witte BI, Buter J, Vergeer MR, Voortman J, Cuijpers P, Leemans CR and Verdonck-de Leeuw IM: The course of symptoms of anxiety and depression from time of diagnosis up to 2 years follow-up in head and neck cancer patients treated with primary (chemo)radiation. *Oral Oncol* 102: 104576, 2020.
- Hidalgo DA: Fibula free flap: A new method of mandible reconstruction. *Plast Reconstr Surg* 84: 71-79, 1989.
- Swartz WM, Banis JC, Newton ED, Ramasastry SS, Jones NF and Acland R: The osteocutaneous scapular flap for mandibular and maxillary reconstruction. *Plast Reconstr Surg* 77: 530-545, 1986.
- Petrovic I, Panchal H, Franca PDDS, Hernandez M, McCarthy CC and Shah J: A Systematic review of validated tools assessing functional and aesthetic outcomes following fibula free flap reconstruction of the mandible. *Head Neck* 41: 248, 2019.
- Ghai S, Sharma Y, Jain N, Satpathy M and Pillai AK: Use of 3-D printing technologies in craniomaxillofacial surgery: A review. *Oral Maxillofac Surg* 22: 249-259, 2018.
- Ritschl LM, Kilbertus P, Grill FD, Schwarz M, Weitz J, Nieberler M, Wolff KD and Fichter AM: In-house, open-source 3D-software-based, CAD/CAM-planned mandibular reconstructions in 20 consecutive free fibula flap cases: An explorative cross-sectional study with three-dimensional performance analysis. *Front Oncol* 11: 731336, 2021.
- Serrano C, van den Brink H, Pineau J, Prognon P and Martelli N: Benefits of 3D printing applications in jaw reconstruction: A systematic review and meta-analysis. *J Craniomaxillofac Surg* 47: 1387-1397, 2019.
- Nyirjesy SC, Heller M, von Windheim N, Gingras A, Kang SY, Ozer E, Agrawal A, Old MO, Seim NB, Carrau RL, *et al*: The role of computer aided design/computer assisted manufacturing (CAD/CAM) and 3-dimensional printing in head and neck oncologic surgery: A review and future directions. *Oral Oncol* 132: 105976, 2022.
- Berrone M, Crosetti E, Tos PL, Pentenero M and Succo G: Fibular osteofasciocutaneous flap in computer-assisted mandibular reconstruction: Technical aspects in oral malignancies. *Acta Otorhinolaryngol Ital* 36: 469-478, 2016.
- Sharma N, Aghlmandi S, Cao S, Kunz C, Honigmann P and Thieringer FM: Quality characteristics and clinical relevance of in-house 3D-printed customized polyetheretherketone (PEEK) implants for craniofacial reconstruction. *J Clin Med* 9: 2818, 2020.
- Christensen R: 'Ordinal-regression models for ordinal data.' R Package Version: 12-10, 2019.
- Heinze G and Schemper M: A solution to the problem of separation in logistic regression. *Stat Med* 21: 2409-2419, 2002.
- Hoene G, Gruber RM, Leonhard JJ, Wiechens B, Schminke B, Kauffmann P, Schliephake H and Brockmeyer P: Combined quality of life and posttraumatic growth evaluation during follow-up care of patients suffering from oral squamous cell carcinoma. *Mol Clin Oncol* 15: 189, 2021.
- Iglesias-Martín F, Oliveros-López LG, Fernández-Olavarría A, Serrera-Figallo MA, Gutiérrez-Corrales A, Torres-Lagares D and Gutiérrez-Pérez JL: Advantages of surgical simulation in the surgical reconstruction of oncological patients. *Med Oral Patol Oral Cir Bucal* 23: e596-e601, 2018.
- Brown JS, Lowe D, Kanatas A and Schache A: Mandibular reconstruction with vascularised bone flaps: A systematic review over 25 years. *Br J Oral Maxillofac Surg* 55: 113-126, 2017.
- Hollows P, McAndrew PG and Perini MG: Delays in the referral and treatment of oral squamous cell carcinoma. *Br Dent J* 188: 262-265, 2000.
- Huang SH, Hahn E, Chiosea SI, Xu ZY, Li JS, Shen L and O'Sullivan B: The role of adjuvant (chemo-)radiotherapy in oral cancers in the contemporary era. *Oral Oncol* 102: 104563, 2020.
- Lee H, Roh JL, Cho KJ, Choi SH, Nam SY and Kim SY: Number of positive lymph nodes better predicts survival for oral cavity cancer. *J Surg Oncol* 119: 675-682, 2019.
- Kim J, Shin ES, Kim JE, Yoon SP and Kim YS: Neck muscle atrophy and soft-tissue fibrosis after neck dissection and postoperative radiotherapy for oral cancer. *Radiat Oncol J* 33: 344-349, 2015.
- Dean A, Alamillos F, Heredero S, Redondo-Camacho A, Guler I and Sanjuan A: Fibula free flap in maxillomandibular reconstruction. Factors related to osteosynthesis plates' complications. *J Craniomaxillofac Surg* 48: 994-1003, 2020.
- López-Arcas JM, Arias J, Del Castillo JL, Burgueño M, Navarro I, Morán MJ, Chamorro M and Martorell V: The fibula osteomyocutaneous flap for mandible reconstruction: A 15-year experience. *J Craniomaxillofac Surg* 68: 2377-2384, 2010.
- van Gemert JTM, Abbink JH, van Es RJJ, Rosenberg AJWP, Koole R and Van Cann EM: Early and late complications in the reconstructed mandible with free fibula flaps. *J Surg Oncol* 117: 773-780, 2018.
- Al-Bustani S, Austin GK, Ambrose EC, Miller J, Hackman TG and Halvorson EG: Miniplates versus reconstruction bars for oncologic free fibula flap mandible reconstruction. *Ann Plast Surg* 77: 314-317, 2016.

26. Wurm MC, Hagen J, Nkenke E, Neukam FW and Schlittenbauer T: The fitting accuracy of pre-bend reconstruction plates and their impact on the temporomandibular joint. *J Craniomaxillofac Surg* 47: 53-59, 2019.
27. Rommel N, Kesting MR, Rohleder NH, Bauer FMJ, Wolff KD and Weitz J: Mandible reconstruction with free fibula flaps: Outcome of a cost-effective individual planning concept compared with virtual surgical planning. *J Craniomaxillofac Surg* 45: 1246-1250, 2017.
28. Tarsitano A, Battaglia S, Crimi S, Ciocca L, Scotti R and Marchetti C: Is a computer-assisted design and computer-assisted manufacturing method for mandibular reconstruction economically viable? *J Craniomaxillofac Surg* 44: 795-799, 2016.
29. Barr ML, Haveles CS, Rezzadeh KS, Nolan IT, Castro R, Lee JC, Steinbacher D and Pfaff MJ: Virtual surgical planning for mandibular reconstruction with the fibula free flap: A systematic review and meta-analysis. *Ann Plast Surg* 84: 117-122, 2020.
30. Geusens J, Sun Y, Luebbbers HT, Bila M, Darche V and Politis C: Accuracy of Computer-aided design/computer-aided manufacturing-assisted mandibular reconstruction with a fibula free flap. *J Craniofac Surg* 30: 2319-2323, 2019.
31. Schepers RH, Raghoobar GM, Vissink A, Stenekes MW, Kraeima J, Roodenburg JL, Reintsema H and Witjes MJ: Accuracy of fibula reconstruction using patient-specific CAD/CAM reconstruction plates and dental implants: A new modality for functional reconstruction of mandibular defects. *J Craniomaxillofac Surg* 43: 649-657, 2015.
32. Moe J, Foss J, Herster R, Powell C, Helman J, Ward BB and VanKoeveering K: An in-house computer-aided design and computer-aided manufacturing workflow for maxillofacial free flap reconstruction is associated with a low cost and high accuracy. *J Craniomaxillofac Surg* 79: 227-236, 2021.



Copyright © 2023 Hoene et al. This work is licensed under a Creative Commons Attribution-NonCommercial-NoDerivatives 4.0 International (CC BY-NC-ND 4.0) License.